Eur. J. Mineral.
2004, **16**, 801–808

Fe^{2+}-O and Mn^{2+}-O bonding and Fe^{2+}- and Mn^{2+}-vibrational properties in synthetic almandine-spessartine solid solutions: an X-ray absorption fine structure study

ALESSANDRA SANI[1], SIMONA QUARTIERI[2]*, FEDERICO BOSCHERINI[3], GIOVANNI ANTONIOLI[4], ANNE FEENSTRA[5] and CHARLES A. GEIGER[6]

[1]Istituto Nazionale per la Fisica della Materia, Operative Group, Grenoble and European Synchrotron Radiation Facility, BP 220, F-38043 Grenoble, France
[2]Dipartimento di Scienze della Terra, Università di Messina, Salita Sperone 31, I-98166 S. Agata di Messina, Italy
*Corresponding author, e-mail: simonaq@unimo.it
[3]Istituto Nazionale per la Fisica della Materia and Dipartimento di Fisica, Università di Bologna, viale Berti Pichat 6/2, I-40127 Bologna, Italy
[4]Istituto Nazionale per la Fisica della Materia and Dipartimento di Fisica, Università di Parma, viale delle Scienze 7/A, I-43100 Parma, Italy
[5]GeoForschungsZentrum Potsdam, Division 4, Telegrafenberg, D-14473 Potsdam, Germany
[6]Institut für Geowissenschaften, Universität Kiel, Olshausenstr. 40, D-24098 Kiel, Germany

Abstract: X-ray absorption fine structure (XAFS) measurements at the Fe and Mn *K*-edges were undertaken to investigate the Fe^{2+}-O and Mn^{2+}-O bonding and Fe^{2+}- and Mn^{2+}-vibrational properties for a series of synthetic almandine-spessartine, $(Fe,Mn)_3Al_2Si_3O_{12}$, garnet solid solutions. The two end members almandine, $Fe_3Al_2Si_3O_{12}$, and spessartine, $Mn_3Al_2Si_3O_{12}$, and three solid solutions of composition Alm75Sps25, Alm50Sps50 and Alm25Sps75 were studied at different temperatures between 77 K and 423 K. The spectra show that the state of alternating bonds provides an appropriate description for the two crystallographically independent X-O(1) and X-O(2) bonds in the solid solution. An exchange of X-site cations in garnet is associated with measurable structural relaxation. The compositional and temperature dependence of the XAFS Debye-Waller factors for Fe^{2+} and Mn^{2+} in the plane of the X-O(1) and the X-O(2) bonds were also determined. Their values in the plane of the X-O(2) bonds are greater compared to those for X-O(1) and they do not vary greatly as a function of garnet composition. In the case of end-member spessartine, the XAFS Debye-Waller factors for Mn^{2+} are compared to the Debye-Waller factors measured from single-crystal X-ray diffraction. An analysis shows correlation in the atomic displacements along the shorter Mn-O(1) bond.

Key-words: garnet, XAFS, silicate solid solutions, local-site distortion, Debye-Waller factor.

Introduction

Garnets are compounds with the general formula $X_3Y_2Z_3O_{12}$. The silicate garnet structure, with Z = Si, can be described as a quasi three-dimensional framework consisting of corner-sharing SiO_4 tetrahedra and YO_6 octahedra, where Y is typically Al, Fe^{3+} or Cr^{3+}. The structure contains a third polyhedron, the XO_8 triangular dodecahedron, in which divalent X-site cations (*e.g.*, Mg, Fe^{2+}, Mn^{2+}, Ca) are located. In nature, garnets occur as multi-component solid solutions consisting of different end members. Here, the aluminosilicate garnets with $Y = Al^{3+}$ are important and they consist of the end members pyrope ($Mg_3Al_2Si_3O_{12}$), grossular ($Ca_3Al_2Si_3O_{12}$), almandine ($Fe_3Al_2Si_3O_{12}$) and spessartine ($Mn_3Al_2Si_3O_{12}$). The crystal-chemical, thermodynamic and physical properties of the aluminosilicate garnets are affected measurably by the chemistry of the X-site cation, and much work has been done to determine these properties for the different end members and also for solid-solution compositions (see Ungaretti *et al.,* 1995; Geiger, 1999, 2004 for reviews).

There is current interest in investigating the atomistic-scale behaviour of silicate solid solutions (Geiger, 2001). A number of issues are important and warrant study and two of them are addressed herein. First, the nature of local bonding behaviour needs investigation. An exchange of different sized X-cations in garnet must lead to atomic and/or unit-cell scale structural distortion and this needs to be measured and quantified. For example, X-O bonding behaviour can be studied to determine whether the virtual crystal approximation (VCA), which assumes a continuous monotonic variation in bond length between end-member components, or the state of alternating

0935-1221/04/0016-0801 $ 3.60
DOI: 10.1127/0935-1221/2004/0016-0801

bonds, which predicts an approximately constant cation-oxygen bond length (Martins & Zunger, 1984; Urusov, 2001), provides a better description for binary aluminosilicate garnet solid solutions (Bosenick *et al.*, 2001; Geiger *et al.,* 2003). The issue is not purely academic in nature, because a correct description is necessary if elastic-strain, thermodynamic (Ganguly *et al.*, 1993; Bosenick *et al.*, 2000; Bosenick *et al.*, 2001) and trace-element substitution (van Westrenen *et al.*, 2003) behaviour in garnet solid solutions are to be understood. Bonding properties and Fe^{2+}-dodecahedral site distortion in Alm-Sps garnets were investigated by single-crystal optical absorption (Geiger & Rossman, 1994) and ^{57}Fe Mössbauer spectroscopy (Geiger *et al.*, 2003). The optical absorption spectra show that Fe^{2+}-dodecahedral distortion and variations in average Fe^{2+}-O bond lengths occur, but the spectroscopic results are difficult to quantify. The Mössbauer results show that the hyperfine parameters associated with the Fe^{2+}-dodecahedral sites are relatively insensitive to local surrounding structural variations. Second, the vibrational behaviour of the X-site cations needs to be determined as a function of garnet composition. Information on their vibration behaviour is important, if one wants to understand the lattice-dynamic and thermodynamic behaviour of garnet solid solutions (*e.g.*, Hofmeister & Chopelas, 1991; Geiger, 1999, 2004). The X-site cations in end-member aluminosilicate garnets have been shown to possess measurable anisotropic amplitudes of vibration (Geiger *et al.*, 1992; Quartieri *et al.*, 1997; Geiger & Ambruster, 1997; Geiger, 2004). Here, the vibrational behaviour of Fe^{2+} in almandine and Mn^{2+} in spessartine as determined by X-ray diffraction can be compared to their behaviour as determined by element-specific spectroscopic methods. Of course, the vibrational behaviour of a specific X-cation in a solid-solution garnet cannot be easily determined by diffraction methods. Here, element-specific spectroscopic measurements need to be employed. Geiger *et al.* (2003) attempted to extract information on the vibrational behaviour of Fe^{2+} in different almandine-bearing binary garnet solid solutions using ^{57}Fe Mössbauer spectroscopy, but this task proved unattainable. The quadrupole split doublet in almandine solid solutions shows subtle variations in asymmetry as a function of garnet composition that is difficult to interpret with respect to the dynamic behaviour of Fe^{2+}. Thus, other spectroscopic methods must be tested to determine if they can yield element-specific vibrational information for the various X-cations in solid-solution compositions.

X-ray absorption fine structure spectroscopy (Lee *et al.*, 1981; Koninsberger & Prins, 1988), XAFS, is an element specific spectroscopic method. It can be used to describe local structural and dynamic properties (site symmetry, interatomic distances, type and number of neighbouring atoms, and Debye-Waller factors) for major, minor and trace elements (for general reviews see: Galoisy, 1996 and Quartieri, 2003; for applications on garnet see: Quartieri *et al.,* 1993, 1995, 1997, 1999a and b, 2002; Mottana *et al.*, 1997; Wu *et al.*, 1996, 1997). XAFS measurements can be used to determine element-specific bond lengths in solid solutions and the vibrational behaviour of selected atoms. Thus, XAFS is well suited to address the two issues for garnet solid solutions discussed above.

In this work, we have chosen to investigate the nature of local Fe^{2+}- and Mn^{2+}-dodecahedral structural properties in a series of synthetic almandine-spessartine solid solutions. In addition, in order to elucidate the vibrational properties of Fe^{2+} and Mn^{2+}, a temperature-dependent study of the Debye-Waller factors was performed between 77 and 423 K for different Alm-Sps compositions.

Experimental methods

The synthesis and characterization of the almandine-spessartine garnets, $(Fe,Mn)_3Al_2Si_3O_{12}$, used in this study have been described in several manuscripts and the relevant information can be obtained therein (Geiger & Feenstra, 1997; Geiger, 1998; Geiger *et al.,* 2003). The samples studied here have the compositions Alm100, Alm75Sps25, Alm50Sps50, Alm25Sps75 and Sps100. For the XAFS measurements, the polycrystalline garnets were finely ground in an agate mortar, dispersed in a solvent using an ultrasound bath and deposed on a Millipore membrane. For the high temperature measurements, the samples were fixed on kapton tape.

The Fe (7112 eV) and Mn (6539 eV) *K*-edge XAFS spectra were collected in transmission mode at the BM08 station of the European Synchrotron Radiation Facility in Grenoble (ESRF, GILDA-CRG) at 77, 100, 200 273, 373 and 423 K. A dynamically sagittally-focussing monochromator with Si(311) crystals (Pascarelli *et al.,* 1996) was used. Harmonics were eliminated by detuning the monochromator crystals. Data were recorded with a spacing of 1 eV in the EXAFS region.

The experimental data (see Fig. 1 for selected examples) were analysed using standard background subtraction and Fourier filtering methods, whereas the determination of structural parameters was carried out using the program FEFFIT (FUSE package; Ravel, 1998). It uses theoretical

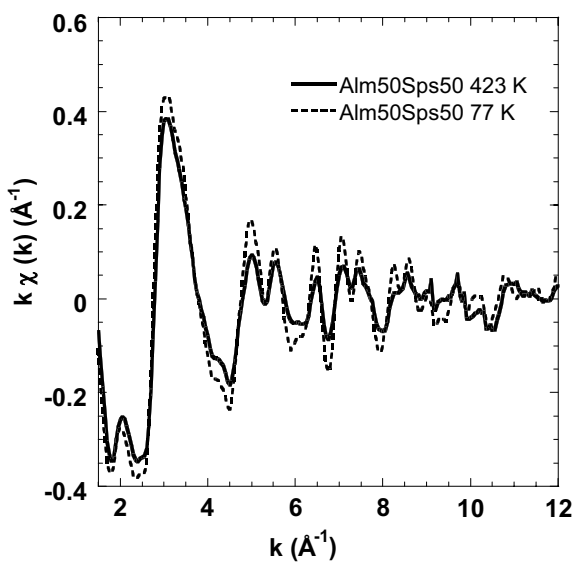

Fig. 1. Iron XAFS signal for the solid solution Alm50Sps50 at two selected temperatures.

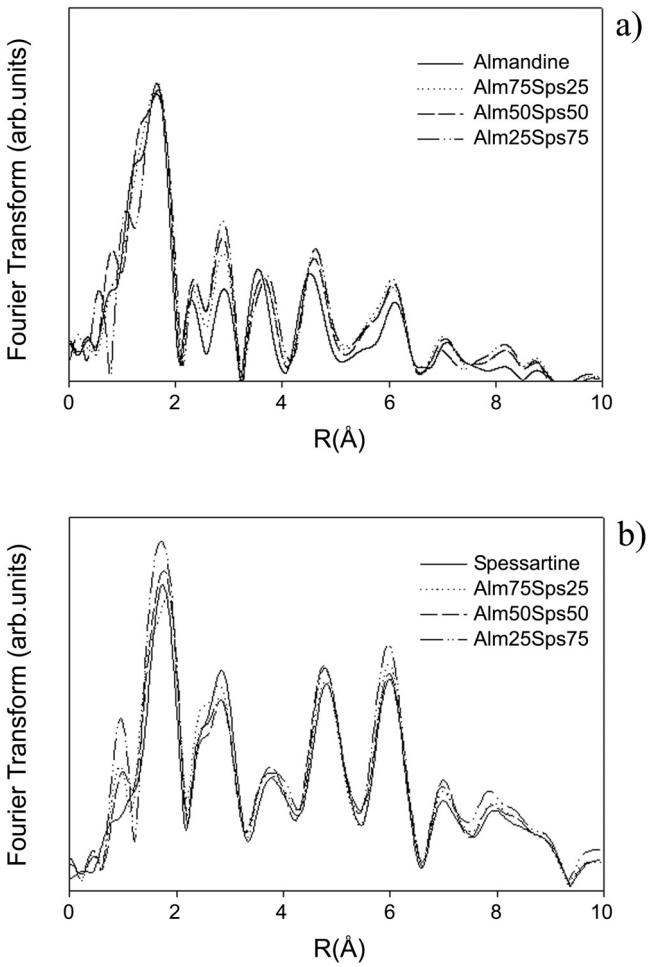

Fig. 2. Modulus of the Fourier transform of $k^2\chi(k)$ as a function of Sps content in garnets at the (a) Fe and (b) Mn edge at 77 K. The first peak reflects the strong overlap of first two Fe^{2+}/Mn^{2+}-O coordination shells. The peaks at higher R-values can be assigned to the outer coordination shells around iron.

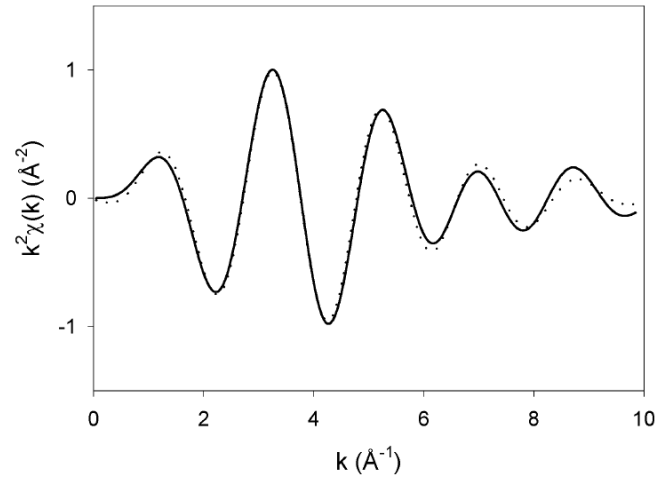

Fig. 3. Fit (dotted) of the back Fourier transform of the data (solid line) of Alm50Sps50 at 77 K (Fe *K*-edge).

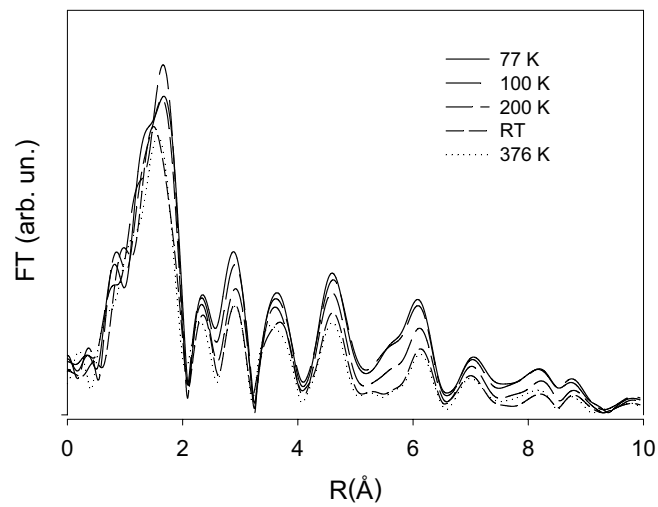

Fig. 4. Modulus of the Fourier transform of $k^2\chi(k)$ at selected temperatures for the sample Alm50Sps50 (Fe edge). The first peak reflects the strong overlap of the first two Fe^{2+}/Mn^{2+}-O coordination shells.

phase functions and amplitudes from FEFF6 software (Rehr *et al.,* 1991; Mustre de Leon *et al.,* 1991). The reliability of the theoretical phases was verified by using Fe_2O_3 and MnO_2 as standards. The dodecahedral site of garnet can be described as a double shell coordination corresponding to the two crystallographically different interatomic X-O distances in the X-site of point symmetry 222. Hence, structural parameters were extracted by a double shell fit of the data. A Fourier transform of the EXAFS signal was performed in the range $k = 2$ to 10 Å^{-1} and an inverse Fourier transform in the range R = 0.9 to 2.1 Å for both Fe and Mn data; fitting was performed in the range $k = 2$ to 10 Å^{-1}. During fitting, the value of the many-body amplitude reduction factor, S_0^2, was fixed to 0.9, the value found from an analysis of the standard compounds. A more sophisticated treatment based upon a cumulant expansion (Bunker, 1983) is of little help in this case because of the strong overlap between the two X-O shells.

Results

The modulus of selected Fourier transforms as a function of garnet composition at the Fe- and Mn *K*-edge edges at 77 K are shown in Fig. 2 a) and b), respectively. The experimental spectra do not show major variations with composition, and we can therefore conclude that Fe^{2+}/Mn^{2+} exchange does not result in major modifications to the garnet structure. We analysed the first two coordination shells, both consisting of 4 oxygen atoms, which overlap in the first peak of the Fourier transform. Fig. 3 shows a typical fit for the sample Alm50Sps50. The results of an XAFS analysis of the Fe and Mn *K*-edge spectra recorded at selected temperatures are reported in Tables 1 and 2, respectively. Fig. 4 shows the Fourier transform for a representative EXAFS signal as a function of temperature for the Fe *K*-edge for the composition Alm50Sps50. One can observe that there are only minor differences between the experimental spectra, which indicate

Table 1. Results of the XAFS analysis at the Fe *K*-edge at different temperatures. The R_{fit} value (normalised sum of the square residuals) refers to the fitting procedure with FEFFIT.

77 K	$\sigma^2_{(Fe\text{-}O(1))}$ (Å^2)	$\sigma^2_{(Fe\text{-}O(2))}$ (Å^2)	$R_{(Fe\text{-}O(1))}$ (Å)	$R_{(Fe\text{-}O(2))}$ (Å)	R_{fit}
Alm	0.006(1)	0.019(3)	2.215(9)	2.338(13)	.02
Alm75Sps25	0.006(1)	0.019(4)	2.218(6)	2.326(8)	.01
Alm50Sps50	0.005(1)	0.019(4)	2.217(9)	2.329(13)	.02
Alm25Sps75	0.006(1)	0.020(4)	2.218(11)	2.326(13)	.02

RT	$\sigma^2_{(Fe\text{-}O(1))}$ (Å^2)	$\sigma^2_{(Fe\text{-}O(2))}$ (Å^2)	$R_{(Fe\text{-}O(1))}$ (Å)	$R_{(Fe\text{-}O(2))}$ (Å)	R_{fit}
Alm	0.009(1)	0.018(3)	2.210(8)	2.357(16)	.02
Alm75Sps25	0.009(2)	0.018(4)	2.213(10)	2.350(19)	.02
Alm50Sps50	0.009(1)	0.017(2)	2.207(7)	2.353(13)	.01
Alm25Sps75	0.009(2)	0.019(4)	2.215(11)	2.350(20)	.03

423 K	$\sigma^2_{(Fe\text{-}O(1))}$ (Å^2)	$\sigma^2_{Fe\text{-}O(2))}$ (Å^2)	$R_{(Fe\text{-}O(1))}$ (Å)	$R_{(Fe\text{-}O(2))}$ (Å)	R_{fit}
Alm75Sps25	0.008(1)	0.022(3)	2.203(5)	2.378(24)	.01
Alm50Sps50	0.008(1)	0.022(4)	2.200(7)	2.376(19)	.02
Alm25Sps75	0.007(1)	0.022(4)	2.194(8)	2.379(20)	.02

Alm data at 423 K are missing due to the sample loss during data collection.

Table 2. Results of the XAFS analysis at the Mn *K*-edge at selected temperatures.

77 K	$\sigma^2_{(Mn\text{-}O(1))}$ (Å^2)	$\sigma^2_{(Mn\text{-}O(2))}$ (Å^2)	$R_{(Mn\text{-}O(1))}$ (Å)	$R_{(Mn\text{-}O(2))}$ (Å)	R_{fit}
Sps	0.006(1)	0.016(3)	2.250(8)	2.405(15)	.02
Alm25Sps75	0.005(1)	0.016(4)	2.255(6)	2.403(19)	.03
Alm50Sps50	0.005(1)	0.017(4)	2.260(8)	2.394(19)	.02
Alm75Sps25	0.004(1)	0.018(4)	2.261(7)	2.388(19)	.02

RT	$\sigma^2_{(Mn\text{-}O(1))}$ (Å^2)	$\sigma^2_{(Mn\text{-}O(2))}$ (Å^2)	$R_{(Mn\text{-}O(1))}$ (Å)	$R_{(Mn\text{-}O(2))}$ (Å)	R_{fit}
Sps	0.006(1)	0.019(4)	2.241(8)	2.426(19)	.03
Alm25Sps75	0.006(1)	0.019(4)	2.239(8)	2.406(20)	.03
Alm50Sps50	0.007(2)	0.019(5)	2.241(10)	2.392(20)	.03
Alm75Sps25	0.006(2)	0.020(5)	2.250(11)	2.375(24)	.03

423K	$\sigma^2_{(Mn\text{-}O(1))}$ (Å^2)	$\sigma^2_{(Mn\text{-}O(2))}$ (Å^2)	$R_{(Mn\text{-}O(1))}$ (Å)	$R_{(Mn\text{-}O(2))}$ (Å)	R_{fit}
Sps	0.009(1)	0.025(4)	2.244(7)	2.407(18)	.02
Alm25Sps75	0.009(1)	0.024(6)	2.238(11)	2.388(27)	.03
Alm50Sps50	0.009(1)	0.023(5)	2.236(9)	2.384(22)	.02
Alm75Sps25	0.008(2)	0.024(7)	2.242(12)	2.392(32)	.04

that variations in structural properties over the investigated temperature range are small. The effect of temperature is most evident in the intensity of the peaks, which decrease with increasing temperature for all coordination shells.

Discussion

X-O bond lengths and site relaxation behaviour

The XAFS Fe^{2+}-O and Mn^{2+}-O bond distances for synthetic end-member almandine and spessartine (Table 1), respectively, are in good agreement with those determined by X-ray diffraction (Geiger *et al.*, 1992; Geiger & Ambruster, 1997).

Fig. 5 shows the Fe^{2+}/Mn^{2+}-O bond distances derived by the XAFS data analysis as a function of Sps content in garnet at 77 K. Several X-ray diffraction studies have been made on garnet solid solutions and diffraction-averaged bond lengths and structural properties have been determined (Armbruster *et al.*, 1992; Ganguly *et al.*, 1993; Ungaretti *et al.*, 1995). However, it is not clear how diffraction-averaged X-O bond lengths, for example, can be interpreted in a physical sense for the case of solid-solution crystals. The diffraction experiment gives averaged X-O lengths that correspond to the VCA description (see, however, Geiger & Armbruster, 1999 for the case where individual element-specific bond lengths were determined). Thus, diffraction-determined bond lengths cannot be directly compared to element-specific bond lengths such as those shown in Fig. 5. The Fe^{2+}-O and Mn^{2+}-O bond lengths given in this plot are element-specific average values, since there could be very slight variations in the bond lengths deriving from different local dodecahedral cation configurations (*i.e.* clusters) that

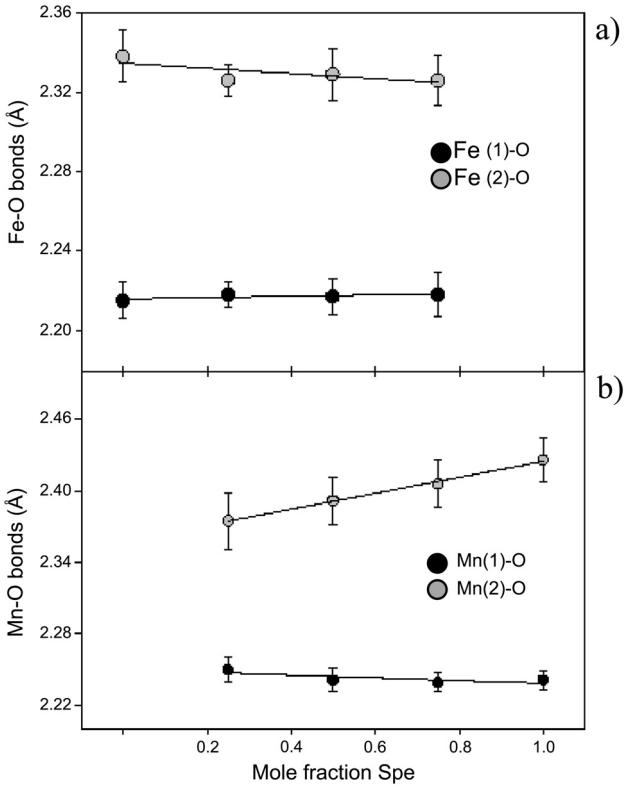

Fig. 5. Bond distances as a function of Sps content at 77 K. (a) Fe edge and (b) Mn edge. The solid line is a linear interpolation.

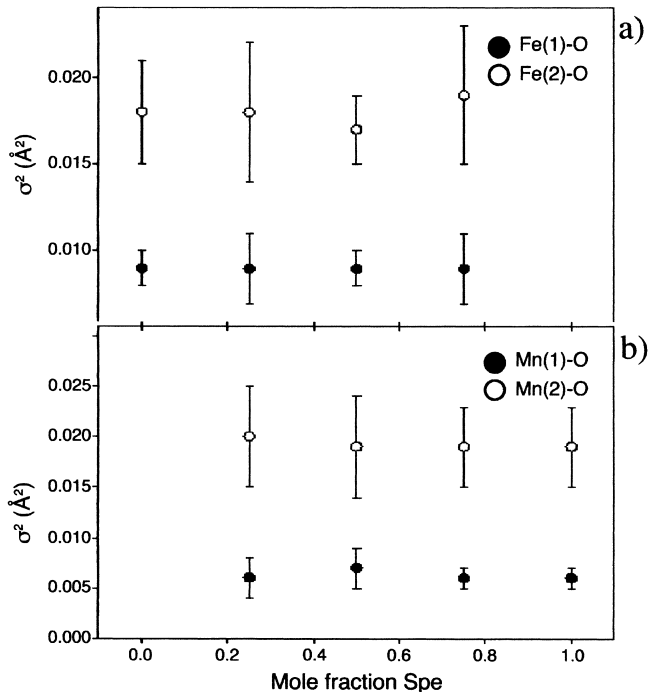

Fig. 6. XAFS Debye-Waller factors as a function of Sps content for the studied samples at room temperature.

can occur in solid-solution compositions (see Geiger, 1999; Geiger *et al.*, 2003). An important point regarding the structural properties of garnets – and other solid-solution systems as well – should be made. When a given X-cation is replaced by another atom, local structure relaxation occurs. Attempts are being made to estimate and even quantify the degree and type of relaxation. It can be described by the element-specific bond lengths, which are measured by XAFS experiments, but not by standard X-ray diffraction experiments.

The XAFS Fe^{2+}-O bond lengths determined here do not vary greatly with garnet composition. However, we note that the longer Fe^{2+}-O bond distance contracts slightly with increasing Sps content, while the longer Mn^{2+}-O bond expands. Hence, the Fe^{2+}- and Mn^{2+}-sites behave in a complementary fashion with changing composition. From these XAFS results we conclude that the state of alternating bonds appears to be an appropriate description for X-O bond behaviour in Alm-Sps solid solutions. This conclusion agrees with structural results obtained from static lattice energy simulations on different binary garnet solid solutions (Bosenick *et al.*, 2000, 2001; van Westrenen *et al.*, 2003) and also ^{57}Fe Mössbauer and electronic energy calculations (Geiger *et al.*, 2003).

Vibrational behaviour of Fe^{2+} and Mn^{2+} as a function of composition and temperature: XAFS *vs* X-ray diffraction data

Contrary to the case for end-member garnets, in studies of solid solutions, X-ray diffraction is generally not capable of delivering vibrational information on an element-specific atom. This can be done though with XAFS. Fig. 6 shows variations in the XAFS Debye-Waller factors, σ^2, for Fe^{2+} and Mn^{2+} at room temperature as a function of Sps content in garnet. The Debye-Waller factor corresponding to the longer X-O(2) bond, σ_2^2, is larger than that of the shorter X-O(1) bond, σ_1^2, for all garnet compositions. The amplitudes of vibration of Fe^{2+} and Mn^{2+} are similar to one another in the plane of the X-O(2) bonds, while in the plane of the X-O(1) bond Fe^{2+} has a larger amplitude of vibration compared to Mn^{2+}. This is in agreement with the X-ray diffraction results (Geiger *et al.,* 1992; Armbruster *et al.,* 1992; Geiger & Armbruster, 1997). Fig. 6 shows, in addition, that the Debye-Waller factors for both cations do not vary greatly as a function of Sps content. The result is consistent with one-mode behaviour observed for phonons with a strong X-cation character in the IR and Raman spectra of Alm-Sps garnets (Geiger, 1998; Kolesov & Geiger, 1998). The Alm-Sps binary shows nearly "ideal" one-mode behaviour in comparison to other binary aluminosilicate garnet solid solutions, where, in comparison, two-mode behaviour is sometimes observed. The physical explanation for one-mode behaviour lies in the similar size and mass of Fe^{2+} and Mn^{2+}, and this is also reflected in the similarity of the XAFS spectra for Alm and Sps.

The Debye-Waller factor corresponding to the longer X-O(2) bond is larger compared to that associated with the X-O(1) bond at all temperatures (Fig. 7). The value of σ_2^2 also more temperature-dependent than that for σ_1^2, which is virtually temperature-independent over the temperature range studied. These results are in agreement with X-ray diffraction results (Geiger *et al.*, 1992; Armbruster *et al.*, 1992;

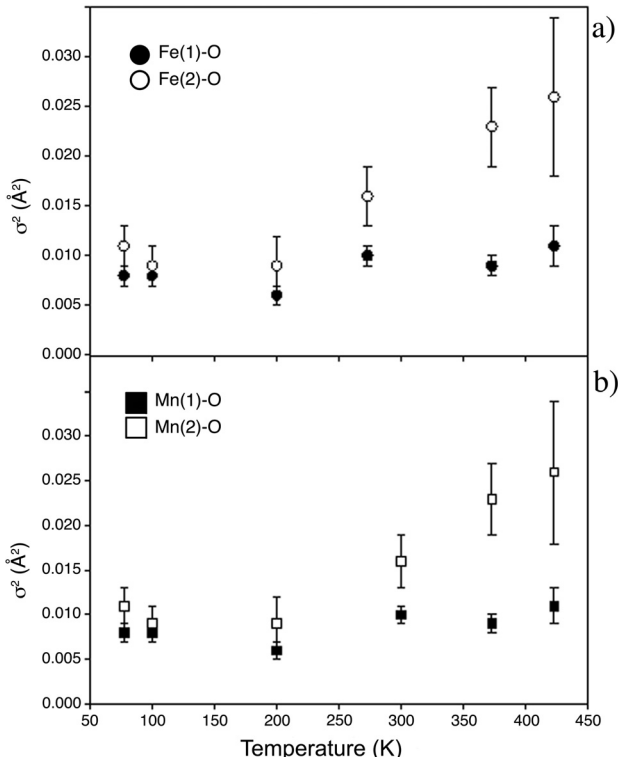

Fig. 7. Temperature dependence of the XAFS Debye-Waller factor, σ^2, in Alm50Sps50. (a) Fe edge and (b) Mn edge.

Geiger & Armbruster, 1997) and Mössbauer spectroscopic measurements (Geiger *et al.*, 1992).

In previous temperature-dependent single-crystal X-ray diffraction studies, the lattice-dynamic properties of end-member almandine and spessartine were investigated between 100 and 500 K (Geiger *et al.,* 1992; Armbruster *et al.,* 1992; Geiger & Armbruster, 1997). Analysis focused on the temperature behaviour of the atomic displacement parameters can be used to determine the dynamic properties of the atoms and polyhedra in the case of ordered end-member garnets. The results show that the SiO_4 tetrahedron and the AlO_6 octahedron can be considered, at least in terms of their diffraction-based vibrational properties, as rigid bodies between 0 K and 500 K. The vibrational behaviour of the XO_8 dodecahedron is different. Unlike the situation for the SiO_4 and AlO_6 polyhedra, the difference atomic displacement parameters along the bonding vectors between the central X-cation and the surrounding oxygen atoms are a function of temperature. It was shown that the Fe^{2+} and Mn^{2+} cations vibrate in an anisotropic manner with their greatest vibrational displacement in the plane of the longer X-O(2) bonds.

Further and complementary information on the vibrational behaviour of the X-cation in garnet can be obtained by XAFS studies. It should be noted, though, that the XAFS Debye-Waller factor is different from that determined by X-ray diffraction (Beni & Platzman, 1976; Greegor & Lytle, 1979; Sevillano *et al.*, 1979). The former is sensitive to short-range correlations in atomic motion, while the latter measures the mean square displacement with respect to the average position of the atom. We refer to the XAFS Debye-Waller factor as the mean square relative displacement (MSRD) between the absorbing and the backscattered atoms, defined as:

$$\sigma_j^2 = \langle(\hat{R}_j \cdot \vec{u}_j)^2\rangle + \langle(\hat{R}_j \cdot \vec{u}_0)^2\rangle - 2\langle(\hat{R}_j \cdot \vec{u}_j) \cdot (\hat{R}_j \cdot \vec{u}_0)\rangle \qquad (1)$$

The first two terms of equation (1) describe the mean square absolute displacement (MSD) of the absorbing and backscattering atoms along the bond direction (*i.e.*, they correspond to the X-ray diffraction displacement parameter) and the third one describes the displacement correlation function. It gives a measure of the in-phase vibrational motion along the bond direction. If this term vanishes, then the two bonded atoms vibrate independently. If, however, the two atoms vibrate together as a unit, the correlation contribution will reduce the amplitude of the XAFS Debye-Waller factor.

Because of the time scale associated with the XAFS process, the XAFS Debye-Waller factor consists of both static (disorder) and vibrational (thermal) components:

$$\sigma^2 = \sigma^2_{\text{static}} + \sigma^2_{\text{vibrational}} \qquad (2)$$

Measurements made at a single temperature do not allow one to separate the two contributions from one another. This can only be done by undertaking experiments at different temperatures. If one adopts a Gaussian pair distribution to describe the atomic position for the absorber and backscatter, and a harmonic approximation to model the vibration, the two contributions are given by:

$$\sigma^2_{\text{static}} = \left\{\sum_{j=1}^{n} (r_j - r_0)^2 \Big/ n\right\} \qquad (3)$$

where r_0 and r_j are the average and the j-th interatomic distances, respectively, and by an Einstein model for the vibration:

$$\sigma^2_{\text{vibrational}} = [h/8\pi^2 m_r v]\coth[hv/2kT] \qquad (4)$$

where m_r is the reduced mass for the atom pair and v is the vibrational frequency.

Thus adopting Eq. (1), a combination of XAFS and X-ray diffraction results can be used to estimate the correlation of motion along an inter-atomic bond, which provides a measure of the in-phase atomic vibrational motion along the bond direction, and to explore its vibrational behaviour and strength. Such an approach was adopted in an investigation of the Fe^{2+}-O bond in almandine (Quartieri *et al.,* 1997) and here it is used again to study the nature of the Mn^{2+}-O bond in spessartine.

A simple comparative discussion of the absolute values of the two different Debye-Waller factors is a difficult task. In both XAFS and X-ray diffraction experiments, a proper determination of their respective Debye-Waller factors is not simple. In both cases a determination is affected by correlation problems with other fit parameters and it can also be affected by how the data analysis was carried out. A correct determination of the XAFS Debye-Waller factor requires that the scattering amplitudes and the scale factor S_0^2 are accounted for properly. In this work, they were obtained by fixing the coordination number of oxygen atoms around the X-cations to eight. In the X-ray diffraction experiments, the atomic displacement parameters are strongly correlated with the site occupancy term in the least-squares refinement procedure and this must be taken into account.

In order to avoid problems in calculating absolute Debye-Waller values in the two techniques, the difference Debye-Waller factors (ΔMSRD, ΔMSD) were used. To do this, the values of the Debye-Waller factors were subtracted by the value corresponding to the lowest temperature attained in each experiment. This is done only for the case of end-member spessartine because X-ray diffraction data are available (Geiger & Armbruster, 1997). Upon making this calculation, one observes a good agreement between ΔMSRD and ΔMSD for the longer Mn^{2+}-O(2) bond as a function of temperature, while for Mn^{2+}-O(1) ΔMSRD is smaller than ΔMSD (Fig. 8). Thus, there is correlated motion along Mn^{2+}-O(1) at room temperature (*i.e.*, there is a considerable in-phase contribution), while along the Mn^{2+}-O(2) bond direction the correlated motion is negligible.

Conclusions

XAFS measurements at the Fe and Mn *K*-edges made on a series of synthetic almandine-spessartine solid solutions permit a determination of their local structural and atomic vibrational properties. The main results can be summarized as follows:

1. Structural variations in X-site geometry as a function of garnet composition are small and are mainly related to a variation in length of the longer Mn^{2+}-O(2) bond distance. The vibrational anisotropy of Fe^{2+} and Mn^{2+} cations in garnet is confirmed and it is only weakly a function of garnet composition.
2. A temperature dependence of the XAFS Debye-Waller factors for Fe^{2+} and Mn^{2+} is observed for all solid-solution compositions. The MSRD along the longer X-O(2) bond is larger and more temperature-dependent than that along the shorter X-O(1) bond.
3. A comparison of the Debye-Waller factors obtained by XAFS and X-ray diffraction for spessartine reveals a negligible contribution of the correlated motion for the longer Mn^{2+}-O(2) bond. The Mn^{2+}-O(1) bond, conversely, is characterized by in-phase motion.

Acknowledgements: The authors acknowledge the financial support of Italian MIUR (COFIN2002 "Geo-cristallochimica degli elementi in traccia") and INFM (Commissione Luce di Sincrotrone). C. A. Geiger's research is supported by DFG grant Ge 649 /14-1. Denis Andrault, P.E. Petit and an anonymous referee are acknowledged for their reviews and useful suggestions that improved the manuscript.

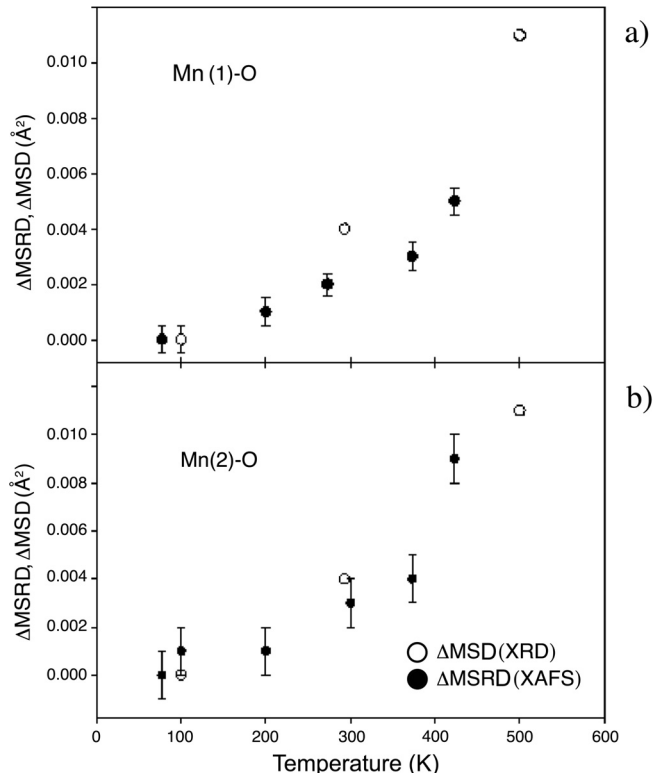

Fig. 8. Temperature dependence of ΔMSRD (filled circles) and ΔMSD (empty circles) for spessartine. (a) Shorter bond Mn^{2+}-O(1), (b) longer bond Mn^{2+}-O(2).

References

Armbruster, T., Geiger, C.A., Lager, G.A. (1992): Single-crystal X-ray structure study of synthetic pyrope almandine garnets at 100 and 293 K. *Am. Mineral.*, **77**, 512-521.

Beni, G. & Platzman, P. (1976): Temperature and polarization dependence of extended X-ray absorption fine structure. *Phys, Rev. B,* **14**, 1514-1518.

Bosenick, A., Dove, M.T., Geiger, C.A. (2000): Simulation studies of pyrope-grossular solid solutions. *Phys. Chem. Minerals*., **27**, 398-418.

Bosenick, A., Dove, M.T., Heine, V., Geiger, C.A. (2001): Scaling of thermodynamic mixing properties in solid solution minerals. *Phys. Chem. Minerals*, **27**, 177-187.

Bunker, G. (1983): Application of the ratio method of EXAFS analysis to disordered systems. *Nucl. Instr. Meth.,* **207**, 437-444.

Galoisy, L. (1996): Local versus average structure around cations in minerals from spectroscopic and diffraction measurements. *Phys. Chem. Minerals,* **23**, 217-225.

Ganguly, J., Cheng, W., ONeill, H.St.C. (1993): Synthesis, volume, and structural changes of garnets in the pyrope-grossular join: Implications for stability and mixing properties. *Am. Mineral*., **78**, 583-593.

Geiger, C.A. (1998): A powder infrared spectroscopic investigation of garnet binaries in the system $Mg_3Al_2Si_3O_{13}$-$Fe_3Al_2Si_3O_{13}$-$Mn_3Al_2Si_3O_{13}$-$Ca_3Al_2Si_3O_{13}$. *Eur. J. Mineral.,* **10,** 407-422.

– (1999): Thermodynamics of $(Fe^{2+}, Mn^{2+}, Mg, Ca)_3Al_2Si_3O_{12}$ garnet: An analysis and review. *Min. Petr.*, **66,** 271-299.

– (2001): Oxide and Silicate Solid Solutions of Geological Importance. *In* "Solid solutions in silicate and oxide systems". EMU Notes Mineral., **3**. Geiger, C.A. (ed.), Eötvös Univ. Press, Budapest, 465 p.

– (2004): Spectroscopic investigations relating to the structural, crystal-chemical and lattice-dynamical properties of $(Fe^{2+}, Mn^{2+}, Mg,Ca)_3Al_2Si_3O_{12}$ garnet: A review and analysis. *In* EMU Notes Mineral., **5**. Libowitsky, E. & Beran, A. (eds.), Eötvös Univ. Press, Budapest, in press.

Geiger, C.A. & Armbruster, T. (1997): $Mn_3Al_2Si_3O_{12}$ spessartine and $Ca_3Al_2Si_3O_{12}$ grossular garnet: structural dynamic and thermodynamic properties. *Am. Mineral.,* **82**, 740-747.

–,– (1999): The crystal structure of a grossular-pyrope garnet solid solution $(Ca_{0.9}Mg_{0.1})_3Al_2(SiO_4)_3$ at 295 and 100 K. *Z. Kristallogr.*, **214,** 211-215.

Geiger, C.A. & Feenstra, A. (1997): Molar volumes of mixing of almandine-pyrope and almandine-spessartine garnets and the crystal chemistry and thermodynamic-mixing properties of aluminosilicate garnets. *Am. Mineral.,* **82**, 571-581.

Geiger, C.A. & Rossman, G.R. (1994): Crystal field stabilization energies of almandine-pyrope and almandine-spessartine garntes determined by FTIR and near infrared measurements. *Phys. Chem. Minerals,* **21**, 516-525.

Geiger, C.A., Armbruster, T., Lager, G.A., Jiang, K., Lottermoser, W., Amthauer, G. (1992): A combined temperature dependent ^{57}Fe Mössbauer and single crystal X-Ray diffraction study of synthetic almandine: evidence for the Gol'danskii-Karyagin effect. *Phys. Chem. Minerals*, **19,** 121-126.

Geiger, C.A., Grodzicki, M., Amthauer, G. (2003): The crystal chemistry and Fe^{II} site properties of aluminosilicate garnet solid solutions as revealed by Mössbauer spectroscopy and electronic structure calculations. *Phys. Chem. Minerals.,* **30**, 280-292.

Greegor, R.B. & Lytle, F.W. (1979): Extended X-ray absorption fine structure determination of thermal disorder in Cu: comparison of theory and experiment. *Phys. Rev B*., **20**, 4902-4907.

Hofmeister, A.M. & Chopelas, A. (1991): Vibrational spectroscopy of end-member silicate garnets. *Phys. Chem. Minerals*, **17**, 503-526.

Kolesov, B.A. & Geiger, C.A. (1998): Raman spectra of silicate garnets. *Phys. Chem. Minerals,* **25**, 142-151.

Koninsberger, D.C. & Prins, R. (Eds.) (1988): X-ray Absorption. Wiley & Sons, New York.

Lee, P.A., Citrin, P.H., Eisenberger, P., Kincaid, B.M. (1981): Extended X-ray absorption fine structure – its strengths and limitations as structural tool. *Rev. Mod. Phys.,* **53**, 769-806.

Martins, J.L. & Zunger, A. (1984): Bond lengths around isovalent impurities and in semiconductor solid solutions. *Phys. Rev. B*, **30,** 6217-6220.

Mottana, A., Della Ventura, G., Romano, C., Marcelli, A., Cibin, G., Paris, E., Giuli, G. (1997): A XAFS study of pyrope garnets and other minerals. *SSRL Activity Rep*., **7**, 171-173.

Mustre de Leon, J., Rehr, J.J., Zabinsky, S.I., Albers, R.C. (1991): Ab initio curved wave X-ray absorption fine structure. *Phys. Rev. B,* **44**, 4146-4156.

Pascarelli, S., Boscherini, F., D'Acapito, F., Hrdy, J., Meneghini, C., Mobilio, S. (1996): X-ray optics of a dynamical sagittal focussing monochromator on the GILDA beamline at the ESRF. *J. Synchrotron Rad.,* **3**, 147-155.

Quartieri, S. (2003): Synchrotron radiation in the Earth Sciences. *In* "Synchrotron Radiation: Fundamentals, Methodologies And Applications". Mobilio, S. & Vlaic, G. (Eds.), Società Italiana di Fisica, Bologna, pp. 427-448.

Quartieri, S., Antonioli, G., Lottici, P.P., Artioli, G. (1993): X-ray absorption study at the Fe K-edge of garnets from the Ivrea-Verbano zone. *Mineral Mag.,* **57**, 249-256.

Quartieri, S., Chaboy, J., Merli, M., Oberti, R., Ungaretti, L. (1995): Local structural environment of calcium in garnets: a combined structure-refinement and XANES investigation. *Phys. Chem. Minerals,* **22**, 159-169.

Quartieri, S., Antonioli, G., Artioli, G., Geiger, C.A., Lottici, P.P. (1997): A temperature dependent X-ray absorption fine structure study of dynamic X-site disorder in almandine: a comparison with diffraction data. *Phys. Chem. Minerals,* **24**, 200-205.

Quartieri, S., Antonioli, G., Geiger, C.A., Artioli, G., Lottici, P.P. (1999a): XAFS characterization of the structural site of Yb in synthetic pyrope and grossular garnets. *Phys. Chem. Minerals,* **26**, 251-256.

Quartieri, S., Chaboy, J., Antonioli, G., Geiger, C.A. (1999b): XAFS characterization of the structural site of Yb in synthetic pyrope and grossular garnets. II: XANES full multiple scattering calculations at the Yb L_I- and L_{III}-edges. *Phys. Chem. Minerals*, **27**, 88-94.

Quartieri, S., Boscherini, F., Chaboy, J., Dalconi, M.C., Oberti, R., Zanetti, A. (2002): Characterization of trace Nd and Ce site preference and coordination in natural melanites: a combined X-ray diffraction and high-energy XAFS study. *Phys. Chem. Minerals,* **29**, 495-502.

Ravel, B. (1998): Exafs analysis system for Emacs.

Rehr, J.J., Mustre de Leon, J., Zabinsky, S.I., Albers, R.C. (1991): Theroetical X-ray absorption fine structure standards. *J. Am. Chem. Soc.,* **113**, 5135-5140.

Sevillano, E., Meuth, H., Rehr, J.J. (1979): Extended X-ray absorption fine structure Debye-Waller factors. I. Monoatomic Crystals. *Phys. Rev. B*, **20**, 4908-4911.

Ungaretti, L., Leona, M., Merli, M., Oberti, R. (1995): Non-ideal solid-solution in garnet: crystal-structure evidence and modelling. *Eur. J. Mineral*., **7**, 1299-1312.

Urusov, V.S. (2001): The phenomenological theory of solid solutions. *In* "Solid solutions in silicate and oxide systems." EMU Notes Mineral., **3**. Geiger, C.A. (ed.), Eötvös Univ. Press, Budapest, 121-153.

van Westrenen, W., Allan, N.L., Blundy, J.D., Lavrentiev, M.Yu., Lucas, B.R., Purton, J.A. (2003): Trace element incorporation into pyrope-grossular solid solutions: an atomistic simulation study. *Phys. Chem. Minerals,* **30**, 217-229.

Wu, Z., Marcelli, A., Mottana, A., Giuli, G., Paris, E., Seifert, F. (1996): Effects of higher-coordination shells in garnets detected by X-ray-absorption spectroscopy at the Al *K* edge. *Phys. Rev. B*, **54**, 2976-2979.

Wu, Z.Y., Marcelli, A., Mottana, A., Giuli, G., Paris, E. (1997): Comparison of XAS spectra at the Al K edge in garnets to multiple-scattering calculations. *J. de Physique* IV, **7**, 503-504.

Received 31 July 2003
Modified version received 7 May 2004
Accepted 4 June 2004